Superconductivity of Organic Charge-Transfer Salts

Wosnitza, J.;

Originally published:

September 2019

Journal of Low Temperature Physics 197(2019), 250-271

DOI: https://doi.org/10.1007/s10909-019-02230-6

jltp manuscript No.
(will be inserted by the editor)

Superconductivity of organic charge-transfer salts

J. Wosnitza

Received: date / Accepted: date

Abstract 40 years after the discovery of the first organic superconductor the nature of the superconducting state in these materials is still not fully understood. Here, I present an overview on the historical developments and current knowledge on this topic for the quasi-one- and quasi-two-dimensional (2D) organic charge-transfer salts. Thereby, I focus on the prototype materials based on the donor molecules tetramethyltetraselenafulvalene (TMTSF) and bisethylenedithio-tetrathiafulvalene (BEDT-TTF or ET for short). 2D organic superconductors based on the latter molecule are found to show Fulde–Ferrell–Larkin–Ovchinnikov (FFLO) states at high magnetic fields and low temperatures. Thermodynamic and nuclear magnetic resonance data give robust evidence for the existence of this FFLO state with modulated order parameter.

Keywords organic superconductors · nature of superconductivity · FFLO state

1 Introduction

In 1979, besides the report of the first heavy-fermion superconductor [1] by Steglich et al., Jérome and coworkers discovered superconductivity in the first organic crystalline material, $(TMTSF)_2PF_6$ [2]. Thereby, TMSTF is tetramethyltetraselenafulvalene with its molecular structure shown in Fig. 1. Charge-transfer salts based on this molecule are now called Bechgaard salts after Klaus Bechgaard, who was the first to grow such crystals. For $(TMTSF)_2PF_6$, a

Hochfeld-Magnetlabor Dresden (HLD-EMFL) and
Würzburg-Dresden Cluster of Excellence ct.qmat
Helmholtz-Zentrum Dresden-Rossendorf
01328 Dresden, Germany
Tel.: +49-351-2603524
Fax: +49-351-2603531
E-mail: wosnitza@hzdr.de

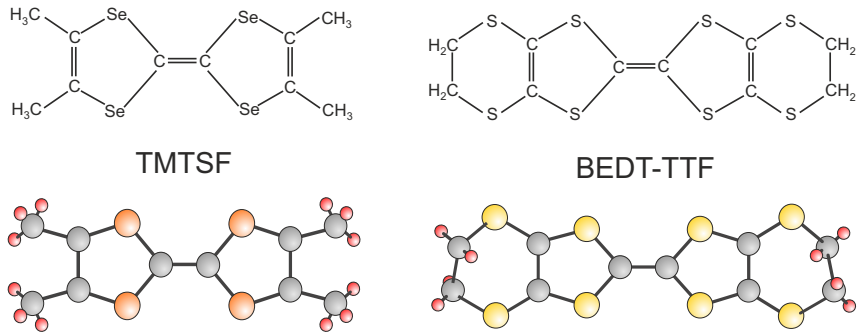

Fig. 1 Molecular structures of (left) tetramethyltetraselenafulvalene (TMTSF) and (right) bisethylenedithio-tetrathiafulvalene (BEDT-TTF or ET for short).

pressure of about 5 to 6 kbar has to be applied to prevent the occurrence of a transition into an insulating spin-density-wave (SDW) state and to allow superconductivity to appear at about $T_c = 1.1$ K. Indeed, the highly anisotropic quasi-one-dimensional (1D) electronic structure leads to Peierls-like metal-insulator transitions for most of the Bechgaard salts [3]. The only exception is $(TMTSF)_2ClO_4$, which becomes superconducting with $T_c = 1.4$ K at ambient pressure [4]. For more detailed introductions into the field of organic superconductors, see [5–9].

Superconductivity in the Bechgaards salts, whether at ambient or applied pressure, is believed to be of unconventional nature. For some time, experimental data suggested triplet pairing in the 1D charge-transfer salts [10,11]. Later, however, this had to be revised since nuclear magnetic resonance (NMR) Knight-shift data evidently rule out such a pairing, at least at low magnetic fields [12]. Consequently, singlet pairing with possible gap nodes is assumed to be present in the 1D organic superconductors. Nonetheless, a possible field-induced transition to triplet superconductivity is discussed as well [13].

Only three years after the discovery of 1D organic superconductors, Parkin and coworkers found superconductivity in a member of a new family of quasi-two-dimensional (2D) materials based on the molecule bisethylenedithio-tetrathiafulvalene (BEDT-TTF or ET for short) [14]. For $(ET)_4(ReO_4)_2$, still pressure was needed to allow superconductivity to appear, but within a few years a large number of ambient-pressure 2D superconductors were found [5,6]. Thereby, most of these 2D charge-transfer salts are based on the ET molecule, or derivatives thereof, such as BETS (= bisethylenedithio-tetrathiafulvalene), with usually a stoichiometry of $(ET)_2X$, where X is a monovalent anion. The ET molecule is shown on the right side of Fig. 1.

Indeed, the $(ET)_2X$ salts are the most intensly investigated class of organic superconductors showing transition temperatures up to 11.5 K at ambient pressure for κ-$(ET)_2Cu[N(CN)_2]Br$ [15], about 13 K for the isostructural material κ-$(ET)_2Cu[N(CN)_2]Cl$ under the moderate pressure of 0.3 kbar [16], and the so-far record 14.2 K for β'-$(ET)_2ICl_2$ under 82 kbar [17]. Thereby, the

prefixes κ and β' label the in-plane arrangement of the ET donor molecules, such as α, β, β'', κ etc. [5,6,18].

Besides superconductivity, the organic charge-transfer salts show a number of remarkable phases, low-temperature states, and non-thermally driven phase transitions. Especially in the 2D κ-phase materials superconductivity competes with antiferromagnetism, with the phases separated by a Mott–Hubbard transition [19,20]. For example, κ-$(ET)_2Cu[N(CN)_2]Cl$ is an antiferromagnetic insulator [21] and κ-$(ET)_2Cu[N(CN)_2]Br$ just on the metallic and superconducting side of the Mott–Hubbard transition. Further to note is the member with $X = Cu_2(CN)_3$ which is on the insulating side of the transition with a large antiferromagnetic exchange interaction, but does not show any long-range order down to lowest temperature; that is, it is the first reported spin-liquid material [22].

There are many similarities between the 2D organic and cuprate high-T_c superconductors [7,8,23–25]. For instance, the conceptual phase diagrams of the organics (see Fig. 2 below) is qualitatively similar to that of the cuprate superconductors, with pressure for the organics equivalent to hole or electron doping for the cuprates. Further, the field-temperature phase diagrams and the vortex dynamics are very similar in both of these layered strongly type-II superconductors. For the 2D organic superconductors, however, there is still no definite experimental proof available, such as phase-sensitive evidence, giving clear-cut evidence for an unconventional pairing symmetry or non-phonon-mediated pairing mechanism [8,18,26]. What is undisputed, is the singlet state of the Cooper pairs in the $(ET)_2X$ salts. However, many experimental data strongly support unconventional pairing with nodes of the order parameter, but as well robust evidence for a fully gapped superconducting state. I will discuss some of the controversial results in the following.

2 Quasi-one-dimensional $(TM)_2X$ salts

Besides the mentioned $(TMTSF)_2X$ Bechgaard salts, isostructural materials based on TMTTF (tetramethyltetrathafulvalene) exist. All of these $(TM)_2X$ salts crystallize in the same triclinic structure with the planar brick-like TM donors forming columnar stacks along the a axis. Along these stacks the short S–S or Se–Se distances lead to a strong molecular-orbital overlap making this the direction of highest conductivity. Along the b and c directions, the overlap is reduced by a factor 10 within the TM layer and by a factor 300 across the anion layers [5,8,13]. These numbers show that the $(TM)_2X$ salts are far from being ideal 1D metals. This non-perfect one dimensionality is, however, exactly what is needed to shift the metal-insulator transition to low temperatures and allows superconductivity to occur at zero or relatively moderate pressures. Indeed, for an ideal one-dimensional metal with a perfectly nested band structure, a Peierls instability leading to an insulating state is inevitable [27].

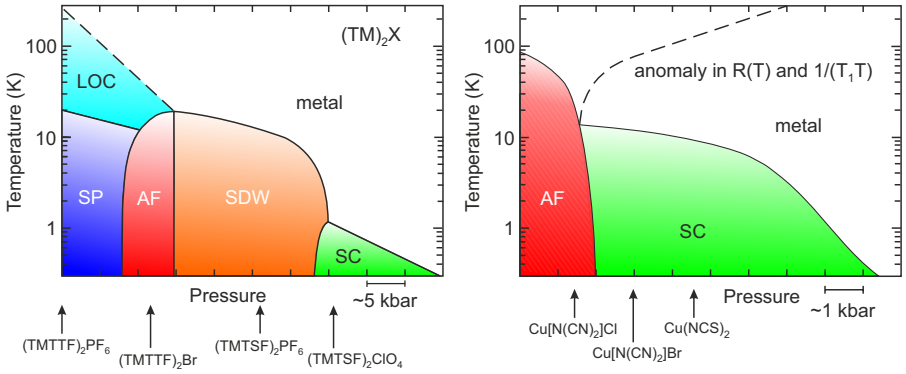

Fig. 2 Schematic temperature-pressure phase diagrams for (left) $(TM)_2X$ salts, where TM stands for TMTTF or TMTSF, and (right) $(ET)_2X$ salts of the κ phase. The arrows indicate ambient-pressure starting points for various materials (for $(ET)_2X$ only the anion x is stated). LOC stands for localized charge carriers, SP for spin Peierls, AF for antiferromagnetism, SDW for spin density wave, and SC for superconductivity.

Depending on the degree of one-dimensionality, different ground states evolve as depicted in the generic pressure-temperature ($P-T$) phase diagram shown in the left panel of Fig. 2 [28]. Thereby, increasing pressure is equivalent to a better overlap of the molecular orbitals which results in larger bandwidths and an increased dimensionality. The TMTTF-based compounds are electronically more one dimensional than the TMTSF analogues. On the far left side of the phase diagram (Fig. 2) $(TMTTF)_2PF_6$ is located. At ambient pressure, an insulating state (LOC) appears already at about 230 K. This is believed to be due to a Mott–Hubbard transition of the strongly correlated electrons. At lower temperatures around 15 K, a spin-Peierls (SP) transition occurs where the antiferromagnetically correlated spin chains condense into a singlet state with a combined lattice distortion [29]. With applying pressure, it is possible to tune $(TMTTF)_2PF_6$ through all the phases shown in Fig. 2 (left panel), with superconductivity appearing at pressures of about 50 kbar. This was shown independently by two groups in sophisticated high-pressure studies [30,31]. These data validate the $P-T$ phase diagram that was originally proposed by Jérome [28].

The nature of the pairing mechanism and the symmetry of the order parameter in the $(TM)_2X$ salts still remains an open question. Early specific-heat data, for example, can be well described within the framework of BCS superconductivity with strong fluctuations due to the low dimensionality [32]. Soon after, however, the notion of conventional superconductivity was questioned. The strong suppression of T_c by nonmagnetic impurities, for instance, indicates a non-s-wave, phase-changing order parameter [33,34]. This, together with the neighboring SDW state led already in the early days to the suggestion of p-wave triplet pairing [35]. Further, proton NMR experiments showed that the spin-lattice relaxation rate, $1/T_1$, in $(TMTSF)_2ClO_4$ decreases roughly with T^3 in the superconducting state [36]. This indicates the presence of line nodes

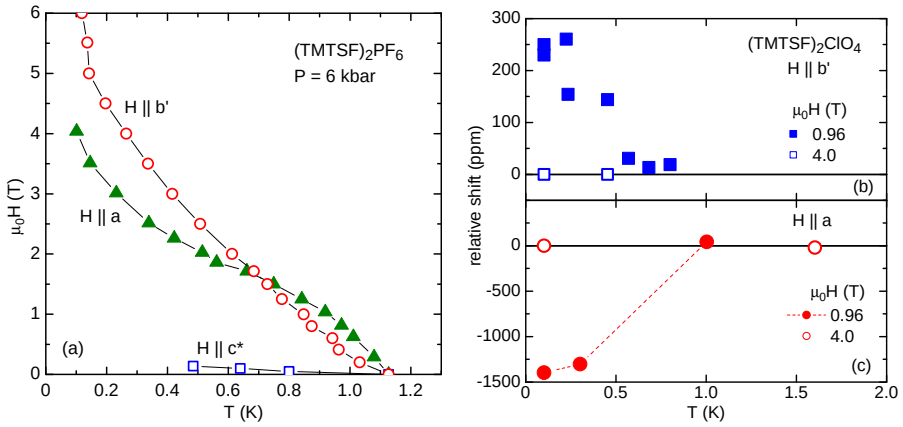

Fig. 3 (a) Resistively determined upper critical fields of $(TMTSF)_2PF_6$ in an applied pressure of 6 kbar and for magnetic fields applied parallel to the highly conducting a and b' directions and, perpendicular, along the least conducting c direction (after Ref. [38]). The right panels show the relative NMR shifts of ^{77}Se spectra of $(TMTSF)_2ClO_4$ at ambient pressure as a functions of temperature for fields applied along the (b) b' and (c) a direction. There is no change observed in 4 T. where the line shift is arbitrarily set to zero (after Ref. [12]).

in the superconducting gap function. In stark contrast, however, later thermal-conductivity measurements evidenced a nodeless gap in the same Bechgaard salt [37].

The notion of unconventional pairing got further support from careful measurements of the anisotropy of the upper critical field, H_{c2}. When aligning the magnetic field in plane, that is, along the a and b' (perpendicular to a) direction, the upper critical fields in $(TMTSF)_2PF_6$ [38] as well as in $(TMTSF)_2ClO_4$ [39] were found to be much larger than the Pauli paramagnetic limit, $\mu_0 H_P = \Delta_0/(\sqrt{2}\mu_B)$, with μ_0 the permeability constant, μ_B the Bohr magneton, and Δ_0 the superconducting energy gap at zero temperature [40,41]. This Pauli limit describes the field when the Zeeman energy becomes larger than the superconducting pairing energy for spin-singlet pairing [42]. For $(TMTSF)_2PF_6$, the Pauli limit was estimated to be about 2.5 T, whereas the resistively determined upper critical in-plane fields lie clearly beyond that value, as shown in Fig. 3(a) [38]. These strongly enhanced H_{c2} motivated the suggestion of spin-triplet pairing in the 1D organic superconductors [43].

This proposal got further support from sophisticated NMR measurements of $(TMTSF)_2PF_6$ with carefully aligned in-plane fields under pressure and dilution-refrigerator temperatures [11,44]. No observable change in the Knight shift of ^{77}Se spectra between the resistively determined normal metallic and superconducting state was found. For singlet pairing with antiparallel spins, a clear drop of the Knight shift, due to the vanishing electron-spin susceptibility, would have been expected. These results stimulated the suggestion of a triplet vector order parameter with spins oriented along the b axis [45] which fits nicely

with the NMR data and is consistent with the mentioned thermal-conductivity results for $(TMTSF)_2ClO_4$ [37].

Subsequently, however, the same group that performed the NMR measurements carefully checked whether the Knight shift may depend on magnetic field. Indeed, for $(TMTSF)_2ClO_4$ they found a clear change of the Knight shift at low magnetic fields [12]. As shown in Fig. 3(b) for field along b' and in Fig. 3(c) for field along a, a clear change of the Knight shift is observed in 0.96 T towards low temperatures when entering the superconducting state. This clearly proves the singlet nature of Cooper pairing. It is, however, not understood why there exists a zero-resistance state at higher fields where the Knight shift remains as in the normal state.

Later, careful angle-resolved specific-heat measurements of $(TMTSF)_2ClO_4$ confirmed the singlet nature of the pairing [46]. These measurements showed a clear Pauli limitation of the bulk upper critical field staying far below the resistive onset of superconductivity. The authors of this work proposed a nodal spin-singlet, possible d-wave order parameter. Somewhat later, however, a low-field muon-spin-rotation study showed no evidence for gap nodes [47]. Instead, an odd-frequency p-wave singlet pairing was suggested. In summary, one has to state that no consensus on the nature of the superconducting state in the 1D charge-transfer salts has been reached. Even conventional s-wave pairing cannot be excluded.

3 Quasi-two-dimensional $(ET)_2X$ salts

3.1 Normal-state properties

Unlike the isostructural 1D $(TM)_2X$ materials, the ET-based charge-transfer salts crystallize in a number of different structures. Due to their twisted ethylene end groups, the ET molecules are not as planar (or brick-like) as the TM donors (see Fig. 1). This allows for a better in-plane overlap of the molecular orbitals and leads to layered 2D structures with less in-plane anisotropy than for the TM salts. The crystal structures mainly differ in the packing motifs of the ET molecules within the layer and are labeled by different Greek letters (see above) [5,18,48].

The common structural feature of most ET-based materials is the packing of the ET molecules into layers which are separated by poorly conducting ("insulating") anion layers, as shown schematically on the right side of Fig. 4. The left side of the figure shows the crystal structure of the 2D organic metal β''-$(ET)_2SF_5CH_2CF_2SO_3$ with especially thick $SF_5CH_2CF_2SO_3^-$ anion layer. The anion layers are sandwiched between the highly conducting ET layers. The sufficiently close contacts between the π orbitals of the sulfur atoms of neighboring in-plane ET molecules results in the formation of 2D molecular bands of typically 0.5 eV width [18]. For the most common $(ET)_2X$ stoichiometry, one electron per two ET donors is transferred to one anion. This leads to partially filled molecular bands, enabling metallic conductivity. The sep-

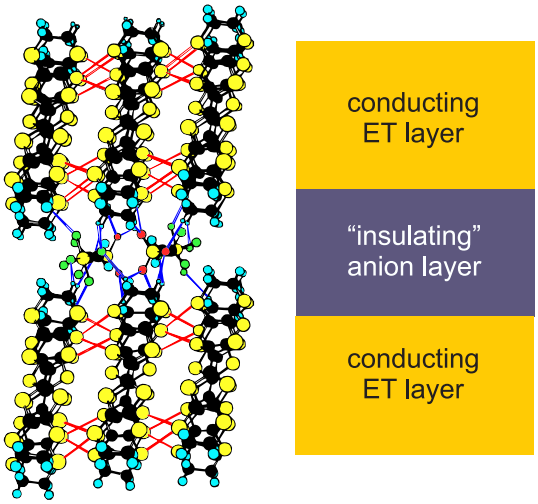

Fig. 4 Crystallographic structure of the 2D organic metal β''-$(ET)_2SF_5CH_2CF_2SO_3$ exemplifying the characteristic alternation of the highly conducting ET layers separated by the poorly conducting (“insulating”) anion layers (schematically shown on the right side).

aration of the ET by the anion layers results in very strong anisotropies of the physical properties parallel and perpendicular to the layers. For instance, the electrical resistivity perpendicular to the layers is 3 to 6 orders of magnitude larger than the in-plane resistivity [5]. The exact value of this anisotropy is, however, difficult to determine since any dislocation disturbs the in-plane transport and leads to an enhanced in-plane resistance [49]. This 2D structure is also reflected in the superconducting properties and resembles that of many layered cuprate superconductors.

The electronic band structure of the ET charge-transfer salts is well known. Depending on the packing motifs of the ET molecules and the corresponding orbital overlaps different in-plane band structures evolve [18, 26]. Remarkably, in spite of the rather complex crystallographic structure with a large number of atoms per unit cell, this in-plane band structure can very well be calculated using the fairly simple extended Hückel tight-binding approximation. Furthermore, the resulting electronic structure is astonishingly simple and, in many cases, resembles a free-electron topology, i.e., a cylindrical Fermi surface with circular cross section. The validity of the calculated Fermi-surface topologies has been favorably verified for most of the ET salts by measurements of magnetic quantum oscillations, such as de Haas–van Alphen (dHvA) and Shubnikov–de Haas (SdH) experiments, as well as angular dependent magnetoresistance oscillations [27, 50, 51]. However, the calculated effective masses are often considerably smaller than the measured values, giving clear evidence for many-body effects which are not included in the band-structure calculations.

The extended-Hückel treatment successfully describes the in-plane electronic band structure, but it does not address the issue of the interlayer band structure. Indeed, for the 2D organic ET salts the interlayer transfer integral, $t_\perp$, often is extremely small and only experimental data were able to provide more information on the degree of three-dimensionality. In case $t_\perp$ is large enough, the resulting corrugation of the Fermi surface can be measured directly. The warped cylindrical Fermi surface leads to two slightly different extremal areas which can be detected, for instance, in dHvA experiments as beating pattern in the magnetic quantum oscillations, such as observed for some β-phase materials [52,53].

For other ET-based metals, however, the question arose whether a real 3D Fermi surface exists. For instance, in β''-$(ET)_2SF_5CH_2CF_2SO_3$ the large separation of the conducting organic layers by the relatively thick anion layers (see Fig. 4) has led to the suggestion that the interlayer transport is "weakly" incoherent [54,55]. Such a scenario of weakly incoherent transport has first been envisioned by McKenzie and Moses [56]. Thereby, the electrons loose their phase information between successive tunneling processes, no Bloch states can evolve, and the band picture breaks down. Indeed, β''-$(ET)_2SF_5CH_2CF_2SO_3$ seems to be such a 2D metal [54,55]. It further shows sawtooth-like dHvA oscillations which follow the behavior expected for an ideal 2D Fermi liquid with fixed chemical potential almost perfectly [57]. Any possible FS corrugation must be extremely small, since dHvA and SdH oscillations start already at about 1.4 T without any indication of beating [58]. As a possible consequence of the weakly incoherent interlayer transport deviations from the conventional Bloch–Boltzmann transport theory and a field-induced metal-insulator transition were observed [59].

3.2 Superconducting properties

The principal superconducting properties of the 2D ET-based metals resemble in many respect the behavior known from the highly anisotropic cuprate superconductors. The organic metals are strongly type-II superconductors with Ginzburg–Landau parameters easily reaching $\kappa_{GL} \approx 100$ for magnetic fields applied perpendicular to the planes. The corresponding extended field range of the Shubnikov phase between the lower and upper critical field, together with the strong anisotropy, leads to rich vortex-dynamics physics; above a certain field, the vortices are free to move and lead to dissipative phenomena and phase diagrams similar to those studied in great detail for the high-T_c materials (for more details see [7,8,18]).

The critical fields of the 2D organic metals depend strongly on the direction of the applied field, as it is expected from the pronounced anisotropy of the electronic band structure. For fields parallel to the ET layers, the lower critical field is considerably smaller than the earth's magnetic field, making it challenging to measure [60]. The slope of the upper critical field at T_c, concomitantly, is extremely steep. An extrapolation of this slope to zero temperature, utiliz-

ing the commonly used temperature dependence [61], yields orbitally limited upper critical fields of some ten tesla. For this field orientation, Pauli-limiting effects become important, as discussed below. This means that the coherence length perpendicular to the layers is much smaller than the layer distance. Consequently, the necessary 3D phase coherence in the superconducting state is established only by Josephson coupling of the superconducting ET layers. Thereby, these layers induce superconductivity in the badly-conducting anion layers, again very similar to the behavior observed in the cuprate superconductors. Evidence for such a scenario has been given by the detection of Josephson plasma resonances in magneto-optical experiments [62].

Another fascinating aspect, worth to be mentioned, is the observation of magnetic-field-induced superconductivity in the Fe-containing BETS salt λ-$(BETS)_2FeCl_4$ [63,64]. For field applied in plane, the material becomes superconducting between about 18 and 41 T. This astonishing observation can be explained by the Jaccarino–Peter field-compensation effect [65]. Thereby, the applied magnetic field becomes compensated by the exchange field that the $S = 5/2$ Fe^{3+} moments exert on the conduction-electron spins. In turn, the internal magnetic field may reach values less than the Pauli paramagnetic limit, thereby allowing the field-induced superconducting state to occur.

3.3 Nature of the superconducting state

Although a definite conclusion on the nature of the superconducting state is still pending, there is clear evidence that the Cooper pairs in the 2D organic charge-transfer salts are in a singlet spin state. This has been shown clearly by NMR experiments [66–68] and by the Pauli-limited upper critical fields that will be discussed below in more detail.

The question on the exchange interaction that mediates Cooper pairing, however, is still a subject of great controversy. Motivated by the $P-T$ phase diagram of the κ-phase materials, shown above in the right panel of Fig. 2, with the proximity of antiferromagnetism next to superconductivity, antiferromagnetic fluctuations were suggested as pairing glue. Maxima found in resistivity and NMR relaxation-rate data above T_c were interpreted as indication for such fluctuations. Indeed, the closeness to the electronically driven Mott-Hubbard transition [19,20] is in line with such a non-phononic pairing mechanism. On the other hand, there is clear experimental evidence for the existence of a considerable electron-phonon coupling in the 2D organic superconductors.

A proof for superconductivity mediated by electron-phonon coupling is the observation of an isotope effect, that is, the change of T_c with varying isotopes. In simplest approximation, BCS theory predicts $T_\mathrm{c} \propto m^{-1/2}$, where m is the isotope mass. Such experiments were done as well for the 2D ET salts. Surprisingly, an inverse isotope effect was found when substituting the eight hydrogen atoms in the ET ethylene end groups by deuterium: T_c was enhanced by about 0.3 K, although a moderate reduction of T_c would have been expected according to the above formula [69]. This effect was explained by a reduced

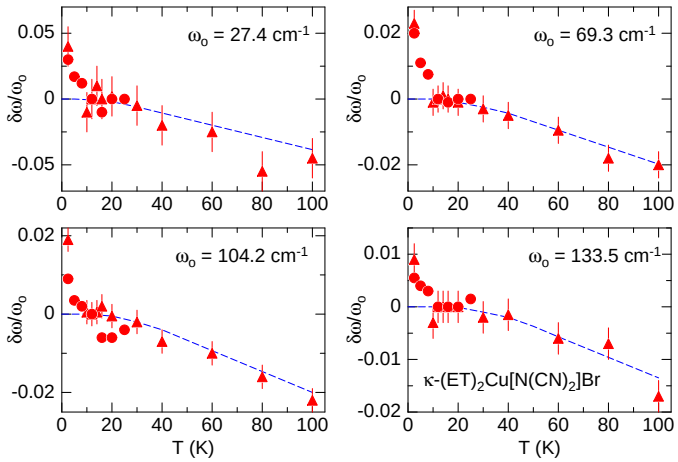

Fig. 5 Temperature dependence of the frequency shifts, $\delta\omega/\omega_0$, of four Raman-active phonon modes in κ-$(ET)_2Cu[N(CN)_2]Br$. The different symbols (triangles and circles) denote two different crystals. The dashed blue curves are calculated taking anharmonicity effects into account (after Ref. [73]).

internal pressure caused by the smaller zero-point displacement of the carbon-deuterium bonds compared to the lighter carbon-hydrogen bonds. In order to avoid this unwanted effect, in another experiment only central atoms in the ET molecules were substituted. When exchanging four ^{12}C atoms by ^{13}C and all eight ^{32}S atoms by ^{34}S, T_c was reduced by about 1%, which agrees well with the BCS expectation [70].

Another experiment that evidenced strong coupling of the lattice to superconductivity utilized inelastic neutron scattering [71]. In κ-(BEDT-TTF)$_2$Cu(NCS)$_2$ below T_c, a large shift of a phonon branch at an energy compatible with the superconducting condensation energy was resolved. The observed shift has hardly been seen so clearly in any other superconductor [71]. (As another example for the direct observation of the superconducting gap in the phonon spectra, see [72].)

Further evidence for a strong influence of superconductivity on various phonon branches was found in Raman-scattering studies. Results of such an investigation for four Raman-active phonon modes are shown in Fig. 5 [73]. For κ-$(ET)_2Cu[N(CN)_2]Br$, a definite hardening of the Raman modes below T_c is found. The dashed curves in Fig. 5 indicate what the typical hardening due to the anharmonic lattice would be if no phase transition would occur. The Raman data show clearly that a significant electron-phonon coupling for various relevant intermolecular phonons exists.

In order to better understand the nature of the superconducting state in the ET-based superconductors as well thermal-conductivity studies were made [74–77]. The result of one of these studies for κ-$(ET)_2Cu[N(CN)_2]Br$ is shown in Fig. 6. Here, contrary to expectations, in the superconducting state higher values of the thermal conductivity, κ, were observed down to lowest

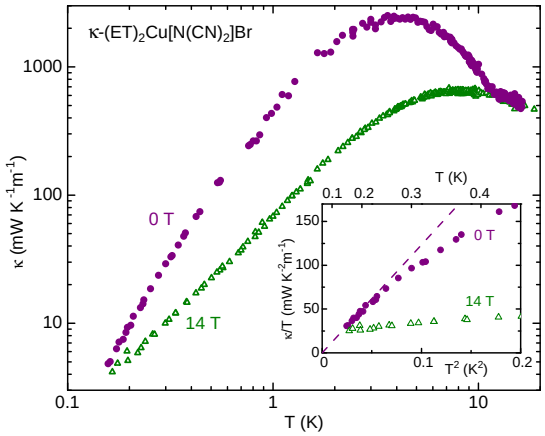

Fig. 6 Temperature dependence of the thermal conductivity, κ, of κ-$(ET)_2Cu[N(CN)_2]Br$ in the superconducting (purple circles in 0 T) and normal state (green triangles in 14 T). The inset shows κ divided by temperature as a function of T^2 down to 160 mK. The dashed line represents a fit to the data between 160 and 220 mK extrapolating to $\kappa = 0$ [77].

temperatures as compared to the normal state. The latter was induced by applying an overcritical magnetic field [77]. Usually, in the superconducting state the thermal conductivity reduces quickly since the electronic contribution to κ diminishes as the quasiparticles condense into Cooper pairs that cannot transport entropy. However, in many novel superconductors a strong increase of κ below T_c is commonly observed as reported for other 2D organic salts [74–76] as well as for heavy-fermion [78] and cuprate superconductors [79]. For the latter high-T_c superconductors a decreasing quasiparticle scattering rate has been suggested as reason for the observed κ enhancement [80]. For the organic superconductors, on the other hand, rather the reduced electron-phonon scattering and, therefore, an increasing phonon mean free path as a result of the Cooper-pair formation is discussed [74,75,77]. Indeed, the better thermal conductivity in the superconducting state of κ-$(ET)_2Cu[N(CN)_2]Br$ shows the dominant phonon contribution to κ down to lowest temperature and evidences strong scattering of the phonons at electrons in the normal state. The inset of Fig. 6 shows a linear fit of κ/T versus T^2 to the data at lowest temperature in the superconducting state. This fit nicely extrapolates to $\kappa/T = 0$, indicating a diminishing electronic contribution to κ and, therefore, a complete superconducting gap without nodes.

All of the above results do not unequivocally prove that the strong electron-phonon coupling is responsible for superconductivity in organic superconductors. Nevertheless, the observed superconducting transitions could well be explained by electron-phonon-mediated Cooper pairing.

Equally controversial as the discussion of the coupling mechanism is the question on the symmetry of the order parameter in the organic superconductors. The experimental situation is rather inconclusive and here mainly some aspects regarding the contradictory results from NMR and specific-heat mea-

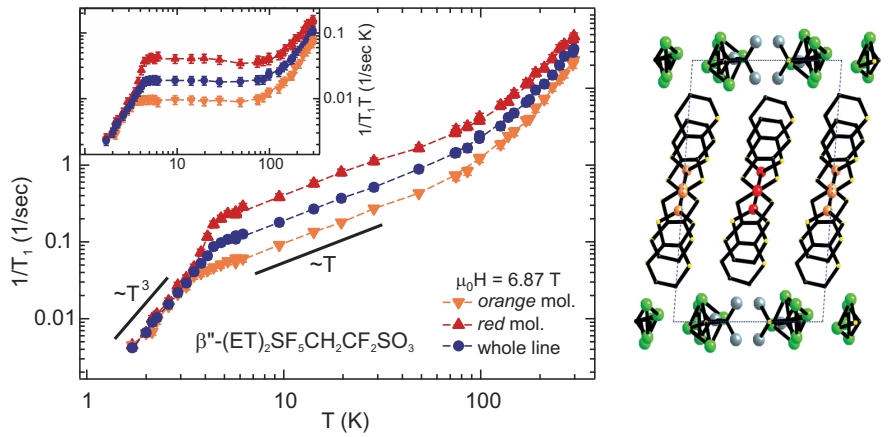

Fig. 7 Temperature dependence of the NMR spin-lattice relaxation rates, $1/T_1$, in β''-$(ET)_2SF_5CH_2CF_2SO_3$ for the "red" and "orange" ET molecules as well as for the whole line (blue). The crystal structure viewed along the stack direction with the ^{13}C spin-labelled ET molecules is shown on the right. The ^{13}C on the bridging sites are colored by red and orange which highlights the crystallographic inequivalence of the two stacks. The inset shows the temperature dependence of $1/(T_1T)$ [83].

surements shall be presented. Further discussion can be found in the reviews [7,8,18,24,49].

An important feature that has to be considered when performing proton NMR investigations of the 2D organic superconductors is the strong enhancement of the spin-lattice relaxation rate, $1/T_1$, below T_c when the magnetic field is not applied parallel to the ET planes [81]. This enhancement is caused by the rapidly changing fields due to flux-line movements which becomes the dominant relaxation channel for the hydrogen nuclei sitting far away from the conduction electrons [82]. In subsequent NMR experiments this was taken into account by applying the magnetic field carefully parallel to the ET planes and using ^{13}C nuclei, i.e., local probes that are placed in the center of the ET molecules and that, therefore, are closely coupled to the itinerant electrons.

A recent example for such an NMR study is shown in Fig. 7. Here, β''-$(ET)_2SF_5CH_2CF_2SO_3$ ($T_c \approx 4.5$ K) with ^{13}C spin-labelled ET molecules at the bridging sites was investigated [83]. The crystal structure with the four inequivalent ^{13}C sites per unit cell, two per ET molecule, is depicted on the right side of Fig. 7. The temperature dependence of the relaxation rates, $1/T_1$, for the different sites with external field oriented in the conducting plane is shown on the left side. The red and orange colors refer to the average for the two sites on each molecule, and the blue points refer to the average of all sites. In the inset $1/(T_1T)$ is plotted, which is expected to be temperature independent for a usual metal. The increase of $1/(T_1T)$ above about 100 K is anomalous, in the sense that the temperature dependence of the susceptibility is too weak to account for the change hinting at temperature-dependent hyperfine coupling. Below 100 K, the expected nearly temperature-independent $1/(T_1T)$ persists

down to T_c. Below that, the relaxation rate drops abruptly without exhibiting a Hebel–Slichter peak, a coherence effect usually observed for s-wave BCS-type superconductors. The data at lowest temperature are compared to a T^3 variation, which commonly is taken as a signature of line nodes of the order parameter, although this is expected only at $T \ll T_c$. A T^3 dependence of $1/(T_1T)$ was as well observed in other correlated superconductors such as the κ-phase organic superconductors [66–68], $(TMTSF)_2X$ [36], as well as cuprate [84] and heavy-fermion superconductors [85,86]. In contrast to these other superconductors, β''-$(ET)_2SF_5CH_2CF_2SO_3$ does not show an enhancement of $1/(T_1T)$ in the normal state that commonly is ascribed to low-energy antiferromagnetic spin fluctuations. This could be taken as an indication for Cooper pairing mediated by charge fluctuations. Indeed, mean-field calculations suggested that the β''-phase materials are prime candidates for such pairing [87]. A test for this hypothesis was suggested to be the constant $1/(T_1T)$ observed in the normal state, unenhanced by spin fluctuations.

Besides NMR, various other experimental data suggest as well the existence of line nodes with possible d-wave pairing symmetry for the 2D organic superconductors. This includes, for example, angle-resolved thermal-conductivity measurements, that revealed a fourfold in-plane symmetry for κ-$(ET)_2Cu(NCS)_2$ being consistent with d-wave pairing [75], as well as a number of scanning-tunnelling spectroscopy studies on the κ-phase ET materials [88–91]. The latter studies agreed on d-wave pairing with either pure $d_{x^2-y^2}$ symmetry [88,89], with d_{xy} component [90], or with the admixture of an extended s-wave pairing leading to an eight-node twofold rotationally symmetric state [91]. It might be worthwhile to note here that, although all these experiments agree on some anisotropic gap structure with presumably d-wave component, they are not phase sensitive and, therefore, cannot verify real zero points of the energy gap.

Contrary to the strong evidence for unconventional pairing symmetries, examples of which are discussed above, most specific-heat experiments show clear evidence for nodeless gaps [92–98]. Indeed, the observation of an exponential vanishing of the electronic part of the specific heat, C_e, in the superconducting state unequivocally rules out any quasiparticle density of states due to nodes in the gap function [18]. As an example, Fig. 8(a) shows the specific heat, C, of β''-$(ET)_2SF_5CH_2CF_2SO_3$ in the superconducting ($\mu_0H = 0$) and normal state with $\mu_0H = 10$ T applied perpendicular to the ET planes [98–100]. The large phonon contribution to the specific heat makes the anomaly at $T_c = 4.3$ K (arrow) hardly visible in the double-logarithmic plot. Anyhow, this anomaly is clearly resolved as shown below in the difference plots [Fig. 9(a)]. In the normal state, below about 2 K, the data are well described by the usual low-temperature approximation of C with a linear electronic and cubic phononic contribution. The obtained Sommerfeld coefficient $\gamma = 19.0(5)$ mJmol^{-1}K^{-2} and Debye temperature of 218(3) K agree well with previous results [95]. The normal-state specific heat together with the knowledge of γ allow to subtract the phonon part from the C data in zero field. The resulting C_e vanishes perfectly according to an exponential function as shown in the normalized plot in

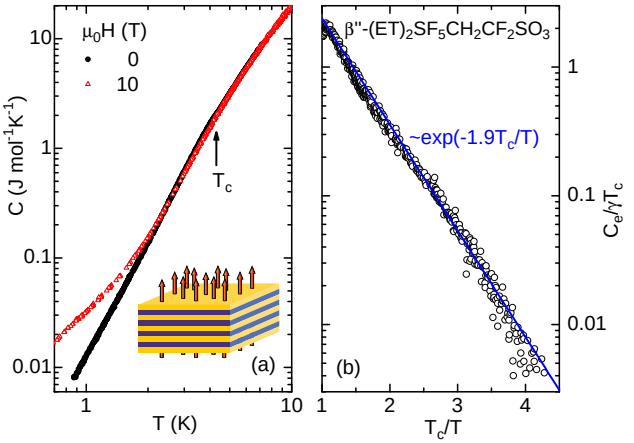

Fig. 8 (a) Specific heat of β''-$(ET)_2SF_5CH_2CF_2SO_3$ vs. temperature in a double-logarithmic plot. Data in the superconducting state at 0 T and in the normal state with $\mu_0 H = 10$ T applied perpendicular to the conducting planes (inset) are shown. (b) Normalized plot of the electronic part of the specific heat, C_e, in the superconducting state divided by γT_c as function of T_c/T. The solid line shows the exponential vanishing of C_e towards low T.

Fig. 8(b). This clear proof for the existence of a complete superconducting gap has been found as well for three other ET-based superconductors by different groups [8,18,92–94,96,97].

In summary, the inconclusive experimental situation, with, on the one side, specific-heat results evidencing nodeless gaps and, on the other side, NMR and other data pointing towards node-like structures prohibits any definitive statement on the nature of superconductivity in the 2D organic charge-transfer salts. It is, however, fair to say, that the specific-heat data are not sensitive to a particular direction and, consequently, cannot resolve any possible gap anisotropy. Therefore, anisotropies as suggested by the mentioned direction-sensitive experiments [75,88–91] may well be present as long as a complete gap finally evolves. In an attempt to solve the puzzling controversy between specific-heat and NMR results, it was suggested that an in-plane magnetic field might induce a transition from an s-wave to d-wave gap symmetry [101].

3.4 Non-uniform superconductivity at high magnetic fields

As outlined above, for magnetic fields applied parallel to the ET layers the slope of the upper critical field at T_c is extremely steep. This reflects the fact that orbital screening currents are very much reduced with the flux lines pinned to the badly conducting anion layers. Consequently, the orbital critical field, H_{orb}, is extraordinarily large and superconductivity is not destroyed by orbital but by spin effects. As mentioned, for fields above the Pauli paramagnetic limit the Zeeman energy becomes larger than the pairing energy and superconductivity for spin-singlet pairing should break down. However, even beyond this

limit superconductivity can survive in special states where the superconducting order parameter is spatially modulated. In 1964, two independent groups, Fulde and Ferrell [102] as well as Larkin and Ovchinnikov [103], predicted the existence of such states, which are now called FFLO states.

At fields above the Pauli limit, BCS-like pairing with zero total momentum is energetically no longer favored. Instead, for FFLO states Cooper pairing with finite center-of-mass momentum is predicted [9,100,104,105]. In real space, this as well leads to an oscillating superconducting order. This "compromise" state allows the material to remain superconducting up to higher magnetic fields by leaving part of its volume in the normal state where the surplus of unpaired spin-up electrons can reside.

Two conditions are necessary to allow the FFLO state to appear. First, the so-called Maki parameter, $\alpha = \sqrt{2}H_{orb}/H_P$ [106], should be larger than 1.8 [107] and, second, clean-limit superconductivity is needed with a mean-free path much larger than the coherence length. These conditions are favorably fulfilled in many ET-based superconductors. As mentioned, the first condition is easily fulfilled for in-plane magnetic fields. Secondly, these materials are clean-limit superconductors as proven by the observance of magnetic quantum oscillations [27,51].

Indeed, there were a number of reports showing indications for the existence of FFLO states in some of the 2D organic metals (see Refs. [100,105] for more details). In most cases, however, the observed features were weak and not solely thermodynamic in nature. The first thermodynamic evidence was reported in 2007 based on specific-heat measurements of κ-$(ET)_2Cu(NCS)_2$ [108]. From these data the temperature-dependent upper critical field was determined revealing a concave curvature at higher temperatures below $T_c = 9.1$ K signalling Pauli limitation. At lower temperatures and higher fields, the curvature changed to convex evidencing the appearance of the FFLO phase. In addition, a second hysteretic anomaly inside the superconducting region was detected [108]. This was originally claimed to signal the transition from the FFLO to the uniform superconducting state, but is now thought to be caused by a small misalignment of the sample [100]. In the following years, a number of additional experiments confirmed the existence of the FFLO state in κ-$(ET)_2Cu(NCS)_2$ and allowed to determine the transition from the uniform to the FFLO superconducting state more reliably. These studies included magnetic-torque magnetization [109], further thermodynamic [110], as well as microscopic NMR experiments [111,112].

In general, FFLO states are expected to exist in many 2D organic superconductors. Some of the materials, however, are available as tiny crystals only or have T_cs that would make it necessary to either perform experiments at very high magnetic fields, not available in usual laboratories, or at mK temperature. β''-$(ET)_2SF_5CH_2CF_2SO_3$, however, has a bulk critical temperature of 4.3 K and Pauli-limiting field of $\mu_0 H_P = 9.73$ T as extracted from the specific-heat data shown in Fig. 8(a) [99]. This allows to investigate a large portion of the superconducting phase diagram in a convenient temperature and field range.

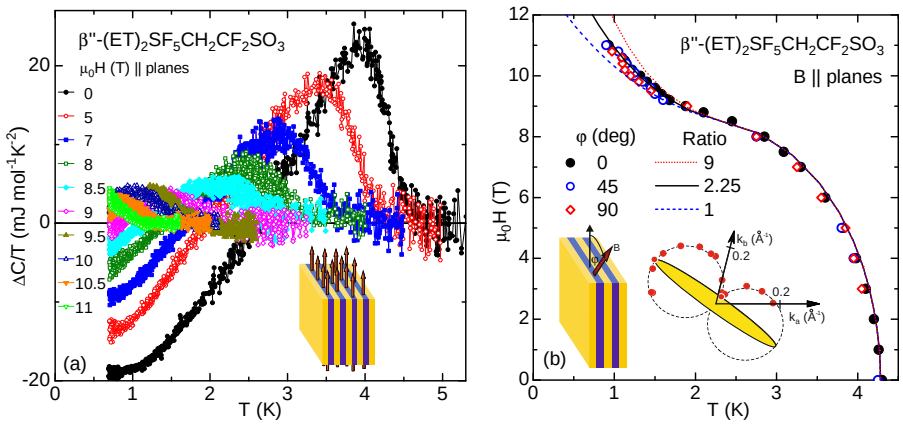

Fig. 9 (a) Temperature dependence of the difference between the specific-heat of β''-$(ET)_2SF_5CH_2CF_2SO_3$ in zero as well as in-plane fields (inset) and the normal-state specific heat, divided by temperature. (b) Field-temperature phase diagram for fields aligned differently within the conducting layers as given by the angle φ (left inset). The data in (a) are taken for $\varphi = 0$. The lines show the calculated upper critical field for different Fermi-velocity ratios of elliptical in-plane Fermi surfaces (see text). The right inset shows the experimentally determined Fermi surface (yellow area) of β''-$(ET)_2SF_5CH_2CF_2SO_3$ with data points (red circles) connected by the dashed line showing the maximal projection of the Fermi wave vector on the field-rotation plane (see Ref. [113] for details).

Besides the measurements in perpendicular field shown in Fig. 8(a), the specific heat of β''-$(ET)_2SF_5CH_2CF_2SO_3$ was measured in a number of fields aligned parallel to the conducting planes with high precision [99]. From these data, the normal-state specific heat [10-T data in perpendicular field shown in Fig. 8(a)] was subtracted. The resulting $\Delta C/T$ as a function of T is shown in Fig. 9(a). From the clearly resolved specific-heat anomalies the field dependence of the critical temperature and the magnetic phase diagram, shown in Fig. 9(b), was extracted. As mentioned, the orbital critical field can be obtained from the initial slope of the critical field at T_c [61] (about -25 T/K) yielding the conservative estimate $\mu_0 H_{orb} \approx 75$ T. This is much larger than $\mu_0 H_P = 9.73$ T and gives a Maki parameter of about 10.9. The steep initial critical-field slope rapidly becomes shallower at higher fields signalling Pauli limitation. The slope steepens again below about 1.8 K, as expected for an emerging FFLO phase.

The field-temperature region where a stable FFLO phase can exist depends on the electronic dimensionality of the material and details of the Fermi surface [100,105]. In general, low-dimensional materials have much larger stability regions than isotropic metals. For 2D metals, this region depends on the in-plane anisotropy of the Fermi surface, or more correctly, on the anisotropy of the Fermi velocity [100]. The upper critical field, calculated using a mean-field treatment for a circular Fermi surface with isotropic in-plane Fermi velocity is shown by the dashed line in Fig. 9(b). Evidently, the measured data are lying above this line which shows that the FFLO state is more stable than this theory

for in-plane isotropy suggests. Indeed, it was shown experimentally [113], that the Fermi surface in β''-$(ET)_2SF_5CH_2CF_2SO_3$ has a highly elliptical shape with an aspect ratio of about 9 [right inset in Fig. 9(b)]. Using a Fermi-velocity ratio of 9 for the calculated phase transition results in the dotted line shown in Fig. 9(b). Now, the experimental data are below the calculated line. This difference between experiment and theory for an aspect ratio of 9 might be explained by the fact that for the calculated phase diagram a simple mean-field description was used neglecting any fluctuations [100]. When using the intermediate ratio of 2.25, the measured data are very well described [solid line in Fig. 9(b)] [100].

Theoretically, it was suggested that the stability region of the FFLO phase should depend on the interplay of the Fermi-surface shape and orbital effects [114]. This question was studied for β''-$(ET)_2SF_5CH_2CF_2SO_3$ by measuring the specific heat for in-plane alignments of the magnetic fields rotated by $\varphi = 45$ and 90 degrees with respect to the original orientation at $\varphi = 0$ shown in Fig. 9(a) [100]. For all in-plane orientations, the extracted phase diagrams fall on top of each other within experimental accuracy. This indicates that the FFLO modulation vector, q, for a state with lowest energy always acquires an optimum direction independent of in-plane field orientation. Most likely the q vector is oriented parallel to the short axis of the in-plane Fermi surface of β''-$(ET)_2SF_5CH_2CF_2SO_3$ [right inset in Fig. 9] allowing to pair the largest number of electrons on the spin-up and spin-down Fermi surfaces with the same q.

In order to obtain microscopic insight into the FFLO state with modulated order parameter, NMR measurements are ideally suited. Thereby, the field-temperature range of the FFLO phase in β''-$(ET)_2SF_5CH_2CF_2SO_3$ allowed for detailed NMR studies using state-of-the-art superconducting magnets and cryostats [83,115,116]. For these studies, the ^{13}C nuclear-spin-labeled crystal already introduced above (Fig. 7) was used. The NMR spectra in the FFLO state were found to be markedly different from the uniform superconducting and from the normal state [115]. With these experiments, the phase diagram obtained by specific heat [Fig. 9(b)] was nicely confirmed and, in addition, the transition line from the uniform superconducting to the FFLO state could be obtained. Besides a considerable broadening of the NMR spectra, their average positions shift strongly and continuously in the FFLO state. A typical spectrum is shown in Fig. 10(a).

In general, the direction of the modulation vector q is not defined and superpositions of different q might be possible. This can lead to various kinds of 1D or 2D order-parameter modulations in the FFLO states [104,105]. A simple approach is to assume a single-q, 1D, sinusoidal modulation that would lead to a spatially oscillating electron-spin polarization as sketched in Fig. 10(c). At the ^{13}C positions in the crystal lattice, therefore, varying local fields lead to corresponding shifts of the NMR spectra. The superposition of all spectra then results in a characteristic double-horn structure for each NMR line [Fig. 10(d)]. In β''-$(ET)_2SF_5CH_2CF_2SO_3$, altogether eight of such broadened NMR lines (four inequivalent crystallographic sites plus dipole coupling) have to be

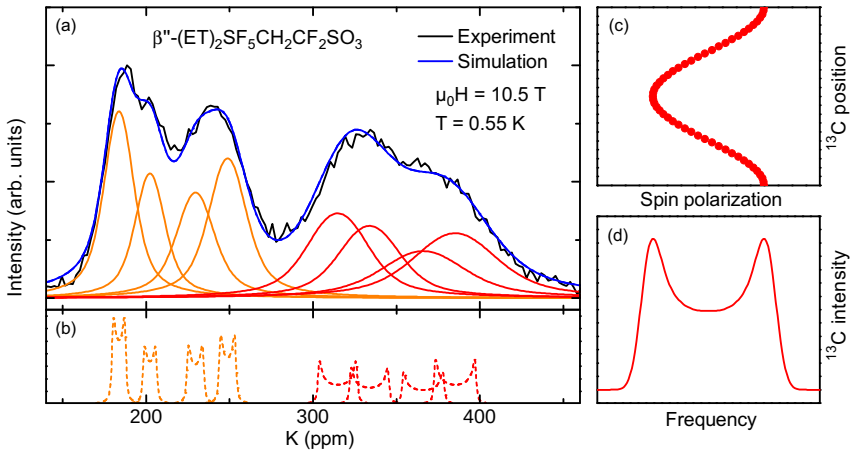

Fig. 10 (a) Experimentally recorded NMR (black) in comparison to the simulated spectrum (blue) generated by assuming a 1D sinusoidal modulation of the electron-spin polarization as shown in (c). This nonuniform spin polarization leads to a characteristic double-horn line shape when convoluted with a Gaussian-broadened NMR spectrum as shown in (d). The red and orange dashed lines in (b) show the resultant NMR lines of the dipole-split ^{13}C NMR signals taking the known hyperfine coupling as scaling factor between spin polarization and NMR frequency into account. For a better visualization of the double-horn structure a Gaussian broadening of only 1 G has been used here. The orange and red lines in (a) depict the eight independent contributions using the real, sample-inherent Gaussian broadening, known from NMR spectra of β''-$(ET)_2SF_5CH_2CF_2SO_3$ in the normal state.

considered. By taking into account the different orbital parts and hyperfine couplings for the independent sites, the NMR lines shown in Fig. 10(b) assuming a Gaussian broadening of only 1 G are obtained. Including the real sample-inherent Gaussian broadening of the lines, the NMR spectrum can be simulated, as shown by the blue line in Fig. 10(a) (red and orange lines). The simulated spectrum agrees very well with the measured one (black line). A description of the data by using a 2D modulated spin polarisation does not fit and can be excluded. Consequently, the NMR data give microscopic evidence for a 1D modulated spin polarization in the FFLO state of the organic superconductor β''-$(ET)_2SF_5CH_2CF_2SO_3$, just as expected for the predicted periodic modulation of the order parameter.

Besides the 2D organic superconductors, there have been some further reports on the appearance of FFLO states in other materials. Prominent examples are a number of heavy-fermion compounds for which, however, the evidence is inconclusive or had to be revised (see Refs. [100,104,105] for more details). In 2003, the heavy-fermion material $CeCoIn_5$ showed thermodynamic evidence for the existence of a second superconducting phase that suggested to claim the existence of the FFLO state [117,118]. Later, neutron-scattering data showed, however, that not the predicted FFLO state, but an incommensurate antiferromagnetic, so-called Q phase, is realized in $CeCoIn_5$ [119].

More recently, FFLO states have been suggested to exist in $CeCu_2Si_2$, the first heavy-fermion superconductor to be studied [120], and in an iron-based superconductor [121]. So far, further support for these claims is missing.

The question remains what the 2D organic superconductors makes so special with respect to the occurrence of FFLO states. An important ingredient certainly is their low dimensionality. Indeed, the stability region of the FFLO state is rather limit in three dimensions and becomes much larger for two-dimensional Fermi surfaces (see [105] and the discussion above on the FFLO stability region for anisotropic 2D Fermi surfaces). Further, the rather simple Fermi-surface topologies and the absence of competing, strong magnetic interactions might favor as well the appearance of FFLO states in the 2D organic charge-transfer salts.

4 Conclusions

In this short review, I presented an overview on some major aspects and current knowledge of the superconductivity in the prototypical 1D and 2D organic charge-transfer salts. Both material classes are strong type-II superconductors with transition temperatures in the few kelvin range for the 1D and up to somewhat above 10 K for the 2D materials. In both cases, strong electronic correlations are important and often magnetic phases are found nearby the superconducting states. For the 1D TMTSF-based materials, triplet superconductivity was discussed for some time. There is, however, now clear evidence that a singlet state is realized in these superconductors. The nature of this state, s, d, or even odd-frequency p wave, is still a matter of debate. The 2D ET-based materials are spin-singlet superconductors as well. The experimental situation with respect to the order-parameter symmetry is highly controversial with evidences in favor for d wave as well as for a fully gapped state. Equally unsettled is, for both material classes, the nature of the coupling mechanism. Spin as well as charge fluctuations have been suggested, but electron-phonon coupling cannot be excluded. Here, phase-sensitive experiments would be highly desirable to settle these open questions.

For some 2D organic $(ET)_2X$ superconductors, there is now solid evidence for the existence of the FFLO state. At low temperatures and for high magnetic field, precisely aligned parallel to the ET layers, thermodynamic experimental data prove the existence of an additional superconducting phase and microscopic NMR measurements show that a periodic modulation of the order parameter exists. Further studies could help to gain a better understanding of this nonuniform superconductivity and to find additional materials evidencing FFLO states with possibly different order-parameter modulations.

Acknowledgements This work was supported by HLD at HZDR, member of the European Magnetic Field Laboratory (EMFL) and by the Deutsche Forschungsgemeinschaft (DFG) through the ANR-DFG grant Fermi-NESt (WO444/13-1).

References

1. F. Steglich, J. Aarts, C. D. Bredl, W. Lieke, D. Meschede, W. Franz, and H. Schäfer, Phys. Rev. Lett. **43**, 1892 (1979).
2. D. Jérome, A. Mazaud, M. Ribault, and K. Bechgaard, J. Physique Lett. **41**, L95 (1980).
3. K. Bechgaard, C. S. Jacobsen, K. Mortensen, J. H. Pederson, and N. Thorup, Solid State Commun. **33**, 1119 (1980).
4. K. Bechgaard, K. Caneiro, M. Olsen, F. B. Rasmussen, and C. S. Jacobsen, Phys. Rev. Lett. **46**, 852 (1981).
5. T. Ishiguro, K. Yamaji, and G. Saito, *Organic Superconductors* (Springer-Verlag, Berlin, Heidelberg, 1998).
6. N. Toyota, M. Lang, and J. Müller, *Low-Dimensional Molecular Metals* (Springer-Verlag, Berlin, 2007).
7. M. Lang and J. Müller, in *Superconductivity*, Vol. II, pp. 1155–1223, K. H. Bennemann and J. B. Ketterson (eds.) (Springer-Verlag, Berlin, Heidelberg, 2008).
8. M. B. Maple, E. D. Bauer, V. S. Zapf, and J. Wosnitza, in *Superconductivity*, Vol. I, pp. 639–762, K. H. Bennemann and J. B. Ketterson (eds.) (Springer-Verlag, Berlin, Heidelberg, 2008).
9. See the articles in *The Physics of Organic Superconductors and Conductors*, A. Lebed (ed.) (Springer-Verlag, Berlin, Heidelberg, 2008).
10. D. Jérome, Chem. Rev. **104**, 5565 (2004).
11. I. J. Lee, S. E. Brown, W. G. Clark, M. J. Strouse, M. J. Naughton, W. Kang, and P. M. Chaikin, Phys. Rev. Lett. **88**, 017004 (2002).
12. J. Shinagawa, Y. Kurosaki, F. Zhang, C. Parker, S. E. Brown, D. Jérome, J. B. Christensen, and K. Bechgaard, Phys. Rev. Lett. **98**, 147002 (2007).
13. A. Ardavan, S. Brown, S. Kagoshima, K. Kanoda, K. Kuroki, H. Mori, M. Ogata, S. Uji, and J. Wosnitza, J. Phys. Soc. Jpn. **81**, 011004 (2012).
14. S. S. P. Parkin, E. M. Engler, R. R. Schumaker, R. Lagier, V. Y. Lee, J. C. Scott, and R. L. Greene, Phys. Rev. Lett. **50**, 270 (1983).
15. A. M. Kini, U. Geiser, H. H. Wang, K. D. Carlson, J. M. Williams, W. K. Kwok, K. D. Vandervoort, J. E. Thompsen, D. L. Stupka, D. Jung, and M. H. Whangbo, Inorg. Chem. **29**, 2555 (1990).
16. J. M. Williams, A. M. Kini, H. H. Wang, K. D. Carlson, U. Geiser, L. K. Montgomery, G. J. Pyrka, D. M.Watkins, J. M. Kommers, S. J. Boryschuk, A. V. S. Crouch, W. K. Kwok, J. E. Schirber, D. L. Overmyer, D. Jung, and M. H. Whangbo, Inorg. Chem. **29**, 3272 (1990).
17. H. Taniguchi, M. Miyashita, K. Uchiyama, K. Satoh, N. Mori, H. Okamoto, K. Miyagawa, K. Kanoda, M. Hedo, and Y. Uwatoko, J. Phys. Soc. Jpn. **72**, 468 (2003).
18. J. Wosnitza, J. Low Temp. Phys. **146**, 641 (2007).
19. H. Kino and H. Fukuyama: J. Phys. Soc. Jpn. **64**, 2726 (1995); H. Kino and H. Fukuyama: J. Phys. Soc. Jpn. **65**, 2158 (1996).
20. K. Kanoda, Hyperfine Interact. **104**, 235 (1997); Physica C **282-287**, 299 (1997).
21. U. Welp, S. Fleshler, W. K. Kwok, G. W. Crabtree, K. D. Carlson, H. H. Wang, U. Geiser, J. M. Williams, and V. M. Hitsman, Phys. Rev. Lett. **69**, 840 (1992).
22. Y. Shimizu, K. Miyagawa, K. Kanoda, M. Maesato, and G. Saito: Phys. Rev. Lett. **91**, 107001 (2003); Y. Shimizu, K. Miyagawa, K. Kanoda, M. Maesato, and G. Saito: Phys. Rev. B **73**, 140407 (2006).
23. R. H. McKenzie, Science **278**, 820 (1997); R. H. McKenzie, Comments Cond. Mat. Phys. **18**, 309 (1998).
24. J. Wosnitza, Physica C **317-318**, 98 (1999).
25. J. Wosnitza, J. Low Temp. Phys. **117**, 1701 (1999).
26. J. Wosnitza, Crystals **2**, 248 (2012).
27. J. Wosnitza, *Fermi Surfaces of Low-Dimensional Organic Metals and Superconductors* (Springer-Verlag, Berlin, 1996).
28. D. Jérome, Science **252**, 1509 (1991).
29. J. P. Pouget, R. Moret, R. Comès, K. Bechgaard, J. M. Fabre, and L. Giral, Mol. Cryst. Liq. Cryst. **79**, 129 (1982).

30. T. Adachi, E. Ojima, K. Kato, H. Kobayashi, T. Miyazaki, M. Tokumoto, and A. Kobayashi, J. Am. Chem. Soc. **122**, 3238 (2000).
31. D. Jaccard, H. Wilhelm, D. Jérome, J. Moser, C. Carcel, and J. M. Fabre, J. Phys.: Condens. Mat. **13**, L89 (2001); H. Wilhelm, D. Jaccard, R. Duprat, C. Bourbonnais, D. Jérome, J. Moser, C. Carcel, and J. M. Fabre, Eur. Phys. J. B **21**, 175 (2001).
32. P. Garoche, R. Brusetti, D. Jérome, and K. Bechgaard, J. Physique Lett. **43**, L147 (1982).
33. M. Y. Choi, P. M. Chaikin, S. Z. Huang, P. Haen, E. M. Engler, and R. L. Greene, Phys. Rev. B **25**, 6208 (1982).
34. N. Joo, P. Auban-Senzier, C. R. Pasquier, D. Jérome, and K. Bechgaard, Europhys. Lett. **72**, 645 (2005).
35. A. A. Abrikosov, J. Low Temp. Phys. **53**, 359 (1983).
36. M. Takigawa, H. Yasuoka, and G. Saito, J. Phys. Soc. Jpn. **56**, 873 (1987).
37. S. Belin and K. Behnia, Phys. Rev. Lett. **79**, 2125 (1997).
38. I. J. Lee, M. J. Naughton, G. M. Danner, and P. M. Chaikin, Phys. Rev. Lett. **78**, 3555 (1997).
39. J. I. Oh and M. J. Naughton, Phys. Rev. Lett. **92**, 067001 (2004).
40. A. K. Clogston, Phys. Rev. Lett. **9**, 266 (1962).
41. B. S. Chandrasekhar, Appl. Phys. Lett. **1**, 7 (1962).
42. In this derivation spin-orbit coupling was neglected, which is an appropriate assumption for the organic superconductors discussed here. For strong spin-orbit coupling, however, the upper critical field may exceed the simple Pauli limit, see, e.g.: Y. Lu, T. Takayama, A. F. Bangura, Y. Katsura, D. Hashizume, and H. Takagi, J. Phys. Soc. Jpn. **83**, 023702 (2014).
43. A. G. Lebed and K. Yamaji, Phys. Rev. Lett. **80**, 2697 (1998); A. G. Lebed, Phys. Rev. B **59**, R721 (1999).
44. I. J. Lee, D. S. Chow, W. G. Clark, M. J. Strouse, M. J. Naughton, P. M. Chaikin, and S. E. Brown, Phys. Rev. B **68**, 092510 (2003).
45. A. G. Lebed, K. Machida, and M. Ozaki, Phys. Rev. B **62**, R795 (2000).
46. S. Yonezawa, Y. Maeno, K. Bechgaard, and D. Jérome, Phys. Rev. B **85**, 140502(R) (2012).
47. F. L. Pratt, T. Lancaster, S. J. Blundell, and C. Baines, Phys. Rev. Lett. **110**, 107005 (2013).
48. J. M. Williams, J. R. Ferraro, R. J. Thorn, K. D. Carlson, U. Geiser, H. H.Wang, A. M. Kini, and M. H.Whangbo, in *Organic Superconductors: Synthesis, Structure, Properties, and Theory* (Prentice Hall, Englewood Cliffs, 1992).
49. J. Singleton and C. Mielke, Contemp. Phys. **43**, 63 (2002).
50. M. V. Kartsovnik, Chem. Rev. **104**, 5737 (2004).
51. J. Singleton, Rep. Prog. Phys. **63**, 1111 (2000).
52. J. Wosnitza, G. Goll, D. Beckmann, S. Wanka, D. Schweitzer, and W. Strunz, J. Phys. I (France) **6**, 1597 (1996).
53. D. Beckmann, S. Wanka, J. Wosnitza, D. Schweitzer, and W. Strunz, Z. Phys. B **104**, 207 (1997).
54. J. Wosnitza, J. Hagel, J. S. Qualls, J. S. Brooks, E. Balthes, D. Schweitzer, J. A. Schlueter, U. Geiser, J. Mohtasham, R. W. Winter, and G. L. Gard, Phys. Rev. B **65**, 180506(R) (2002).
55. J. Wosnitza, J. Hagel, O. Ignatchik, B. Bergk, V. M. Gvozdikov, J. A. Schlueter, R. W. Winter, and G. L. Gard, J. Low Temp. Phys. **142**, 327 (2006).
56. R. H. McKenzie and P. Moses, Phys. Rev. Lett. **81**, 4492 (1998); P. Moses and R. H. McKenzie, Phys. Rev. B **60**, 7998 (1999).
57. J. Wosnitza, S. Wanka, J. Hagel, E. Balthes, N. Harrison, J. A. Schlueter, A. M. Kini, U. Geiser, J. Mohtasham, R. W. Winter, and G. L. Gard, Phys. Rev. B **61**, 7383 (2000).
58. J. Wosnitza, J. Hagel, P. J. Meeson, D. Bintley, J. A. Schlueter, J. Mohtasham, R. W. Winter, and G. L. Gard, Phys. Rev. B **67**, 060504(R) (2003).
59. J. Wosnitza, S. Wanka, J. Hagel, H. v. Löhneysen, J. S. Qualls, J. S. Brooks, E. Balthes, J. A. Schlueter, U. Geiser, J. Mohtasham, R. W. Winter, and G. L. Gard, Phys. Rev. Lett. **86**, 508 (2001).
60. S. Wanka, D. Beckmann, J. Wosnitza, E. Balthes, D. Schweitzer, W. Strunz, and H.J. Keller, Phys. Rev. B **53**, 9301 (1996).

61. N. R. Werthamer, E. Helfand, and P. C. Hohenberg, Phys. Rev. **147**, 295 (1966).
62. P. Müller, in *Advances in Solid State Physics* (Vieweg, Braunschweig, 1994).
63. S. Uji, H. Shinagawa, T. Terashima, T. Yakabe, Y. Terai, M. Tokumoto, A. Kobayashi, H. Tanaka, and H. Kobayashi, Nature **410**, 908 (2001).
64. L. Balicas, J. S. Brooks, K. Storr, S. Uji, M. Tokumoto, H. Tanaka, H. Kobayashi, A. Kobayashi, V. Barzykin, and L. P. Gor'kov, Phys. Rev. Lett. **87**, 067002 (2001).
65. V. Jaccarino and M. Peter, Phys. Rev. Lett. **9**, 290 (1962).
66. S. M. D. Soto, C. P. Slichter, A. M. Kini, H. H. Wang, U. Geiser, and J. M. Williams, Phys. Rev. B **52**, 10 364 (1995).
67. H. Mayaffre, P. Wzietek, D. Jérome, C. Lenoir, and P. Batail, Phys. Rev. Lett. **75**, 4122 (1995).
68. K. Kanoda, K. Miyagawa, A. Kawamoto, and Y. Nakazawa, Phys. Rev. B **54**, 76 (1996).
69. A. M. Kini, J. A. Schlueter, B. H. Ward, U. Geiser, and H. H. Wang, Synth. Met. **120**, 713 (2001).
70. A. M. Kini, K. D. Carlson, H. H. Wang, J. A. Schlueter, J. D. Dudek, S. A. Sirchio, U. Geiser, K. R. Lykke, and J. M. Williams, Physica C **264**, 81 (1996).
71. L. Pintschovius, H. Rietschel, T. Sasaki, H. Mori, S. Tanaka, N. Toyota, M. Lang, and F. Steglich, Europhys. Lett. **37**, 627 (1997).
72. F. Weber, A. Kreyssig, L. Pintschovius, R. Heid, W. Reichardt, D. Reznik, O. Stockert, and K. Hradil, Phys. Rev. Lett. **101**, 237002 (2008).
73. D. Pedron, G. Visentini, R. Bozio, J. M. Williams, and J. A. Schlueter, Physica C **276**, 1 (1997).
74. S. Belin, K. Behnia, and A. Deluzet, Phys. Rev. Lett. **81**, 4728 (1998).
75. K. Izawa, H. Yamaguchi, T. Sasaki, and Y. Matsuda, Phys. Rev. Lett. **88**, 027002 (2002).
76. M. A. Tanatar, T. Ishiguro, H. Tanaka, and H. Kobayashi, Phys. Rev. B **66**, 134503 (2002).
77. S. Kühlmorgen, R. Schönemann, E. L. Green, J. Müller, and J. Wosnitza, J. Phys.: Condens. Matter **29**, 405604 (2017).
78. M. A. Tanatar, J. Paglione, S. Nakatsuji, D. G. Hawthorn, E. Boaknin, R. W. Hill, F. Ronning, M. Sutherland, L. Taillefer, C. Petrovic, P. C. Canfield, and Z. Fisk, Phys. Rev. Lett. **95**, 067002 (2005).
79. R. C. Yu, M. B. Salamon, J. P. Lu, and W. C. Lee, Phys. Rev. Lett. **69**, 1431 (1992).
80. K. Krishana, J. M. Harris, and N. P. Ong, Phys. Rev. Lett. **75**, 3529 (1995).
81. F. Creuzet, C. Bourbonnais, D. Jérome, D. Schweitzer, and H. J. Keller, Europhys. Lett. **1**, 467 (1986); F. Creuzet, C. Bourbonnais, G. Creuzet, D. Jérome, D. Schweitzer, and H. J.Keller, Physica B **143**, 363 (1986).
82. S. M. D. Soto, C. P. Slichter, H. H. Wang, U. Geiser, and J. M. Williams, Phys. Rev. Lett. **70**, 2956 (1993).
83. G. Koutroulakis, H. Kühne, H. H. Wang, J. A. Schlueter, J. Wosnitza, and S. E. Brown, arXiv: 1601.06107 (2016).
84. T. Imai, T. Shimizu, H. Yasuoka, Y. Ueda, and K. Kosuge, J. Phys. Soc. Jpn. **57**, 2280 (1988).
85. D. E. MacLaughlin, C. Tien, W. G. Clark, M. D. Lan, Z. Fisk, J. L. Smith, and H. R. Ott, Phys. Rev. Lett. **53**, 1833 (1984).
86. G.-q. Zheng, K. Tanabe, T. Mito, S. Kawasaki, Y. Kitaoka, D. Aoki, Y. Haga, and Y. Onuki, Phys. Rev. Lett. **86**, 4664 (2001).
87. J. Merino and R. H. McKenzie, Phys. Rev. Lett. **87**, 237002 (2001).
88. T. Arai, K. Ichimura, K. Nomura, S. Takasaki, J. Yamada, S. Nakatsuji, and H. Anzai, Phys. Rev. B **63**, 104518 (2001).
89. K. Ichimura, M. Takami, and K. Nomura, J. Phys. Soc. Jpn. **77**, 114707 (2008).
90. Y. Oka, H. Nobukane, N. Matsunaga, K. Nomura, K. Katono, K. Ichimura, and A. Kawamoto, J. Phys. Soc. Jpn. **84**, 064713 (2015).
91. D. Guterding, S. Diehl, M. Altmeyer, T. Methfessel, U. Tutsch, H. Schubert, M. Lang, J. Müller, M. Huth, H. O. Jeschke, R. Valentí, M. Jourdan, and H.-J. Elmers, Phys. Rev. Lett. **116**, 237001 (2016); D. Guterding, M. Altmeyer, H. O. Jeschke, and R. Valentí, Phys. Rev. B **94**, 024515 (2016).
92. H. Elsinger, J. Wosnitza, S. Wanka, J. Hagel, D. Schweitzer, and W. Strunz, Phys. Rev. Lett. **84**, 6098 (2000).

93. J. Wosnitza, S. Wanka, J. Hagel, M. Reibelt, D. Schweitzer, and J.A. Schlueter, Synth. Met. **133-134**, 201 (2003).
94. J. Wosnitza, X. Liu, D. Schweitzer, and H.J. Keller, Phys. Rev. B **50**, 12747 (1994).
95. S. Wanka, J. Hagel, D. Beckmann, J. Wosnitza, J.A. Schlueter, J.M. Williams, P.G. Nixon, R.W. Winter, and G.L. Gard, Phys. Rev. B **57**, 3084 (1998).
96. A.E. Kovalev, T. Ishiguro, J. Yamada, S. Takasaki, and H. Anzai, JETP **92**, 1035 (2001).
97. J. Müller, M. Lang, R. Helfrich, F. Steglich, and T. Sasaki, Phys. Rev. B **65**, 140509(R) (2002).
98. R. Beyer and J. Wosnitza, Low Temp. Phys. **39**, 293 (2013).
99. R. Beyer, B. Bergk, S. Yasin, J. A. Schlueter, and J. Wosnitza, Phys. Rev. Lett. **109**, 027003 (2012).
100. J. Wosnitza, Ann. Phys. **530**, 1700282 (2018).
101. G. Varelogiannis, Phys. Rev. Lett. **88**, 117005 (2002).
102. P. Fulde and R. A. Ferrell, Phys. Rev. **135**, A550 (1964).
103. A. I. Larkin and Y. N. Ovchinnikov, Zh. Eksp. Teor. Fiz. **47**, 1136 (1964) [Sov. Phys. JETP **20**, 762 (1965)].
104. Y. Matsuda and H. Shimahara, J. Phys. Soc. Jpn. **76**, 051005 (2007).
105. G. Zwicknagl and J. Wosnitza in: BCS: 50 years edited by L. N. Cooper and D. Feldman, (World Scientific, Singapore, 2011) p. 337–371; G. Zwicknagl and J. Wosnitza, Int. J. Mod. Phys. B **24**, 3915 (2010).
106. K. Maki and T. Tsuneto, Prog. Theor. Phys. **31**, 945 (1964).
107. L. W. Gruenberg and L. Gunther, Phys. Rev. Lett. **16**, 996 (1966).
108. R. Lortz, Y. Wang, A. Demuer, P. H. M. Böttger, B. Bergk, G. Zwicknagl, Y. Nakazawa, and J. Wosnitza, Phys. Rev. Lett. **99**, 187002 (2007).
109. B. Bergk, A. Demuer, I. Sheikin, Y. Wang, J. Wosnitza, Y. Nakazawa, and R. Lortz, Physica C **470**, 586 (2010); B. Bergk, A. Demuer, I. Sheikin, Y. Wang, J. Wosnitza, Y. Nakazawa, and R. Lortz, Phys. Rev. B **83**, 064506 (2011).
110. C. C. Agosta, N. A. Fortune, S. T. Hannahs, S. Gu, L. Liang, J. Park, and J. A. Schlueter, Phys. Rev. Lett. **118**, 267001 (2017).
111. J. A. Wright, E. Green, P. Kuhns, A. Reyes, J. Brooks, J. Schlueter, R. Kato, H. Yamamoto, M. Kobayashi, and S. E. Brown, Phys. Rev. Lett. **107**, 087002 (2011).
112. H. Mayaffre, S. Krämer, M. Horvatić, C. Berthier, K. Miyagawa, K. Kanoda, and V. F. Mitrovic, Nat. Phys. **10**, 928 (2014).
113. J. Wosnitza, S. Wanka, J. S. Qualls, J. S. Brooks, C. H. Mielke, N. Hanison, J. A. Schlueter, J. M. Williams, P. G. Nixon, R. W. Winter, and G. L. Gard, Synth. Metals, **103**, 2000 (1999).
114. M. D. Croitoru, M. Houzet, and A. I. Buzdin, Phys. Rev. Lett. **108**, 207005 (2012).
115. G. Koutroulakis, H. Kühne, J. A. Schlueter, J. Wosnitza, and S. E. Brown, Phys. Rev. Lett. **116**, 067003 (2016).
116. S. Molatta, PhD thesis 2018, TU Dresden.
117. A. Bianchi, R. Movshovich, C. Capan, P. Pagliuso, and J. Sarrao, Phys. Rev. Lett. **91**, 187004 (2003).
118. H. A. Radovan, N. A. Fortune, T. P. Murphy, S. T. Hannahs, E. C. Palm, S. W. Tozer, and D. Hall, Nature **425**, 51 (2003).
119. M. Kenzelmann, T. Strässle, C. Niedermayer, M. Sigrist, B. Padmanabhan, M. Zolliker, A. D. Bianchi, R. Movshovich, E. D. Bauer, J. L. Sarrao, and J. D. Thompson, Science **321**, 1652 (2008).
120. S. Kitagawa, G. Nakamine, K. Ishida, H. S. Jeevan, C. Geibel, and F. Steglich, Phys. Rev. Lett. **121**, 157004 (2018).
121. C. Cho, J. H. Yang, N. F. Q. Yuan, J. Shen, T. Wolf, and R. Lortz, Phys. Rev. Lett. **119**, 217002 (2017).